European Journal of Pharmaceutics and Biopharmaceutics 77 (2011) 376–383

Contents lists available at ScienceDirect

European Journal of Pharmaceutics and Biopharmaceutics

journal homepage: www.elsevier.com/locate/ejpb

Research paper

Interaction of metal oxide nanoparticles with lung surfactant protein A

Christine Schulze [a], Ulrich F. Schaefer [a], Christian A. Ruge [a], Wendel Wohlleben [b], Claus-Michael Lehr [a,c,*]

[a] Department of Biopharmaceutics and Pharmaceutical Technology, Saarland University, Saarbruecken, Germany
[b] BASF SE, Polymer Physics Research, GKP/O – G201, Ludwigshafen, Germany
[c] Department of Drug Delivery (DDEL) Helmholtz-Institute for Pharmaceutical Research Saarland (HIPS) Helmholtz Center for Infection Research (HZI), Saarland University, Campus A 4 1, Saarbruecken, Germany

ARTICLE INFO

Article history:
Available online 5 November 2010

Keywords:
Surfactant protein A
Nanoparticles
Particle–protein interaction
Protein adsorption
Deagglomeration
BCA assay

ABSTRACT

The alveolar lining fluid (ALF) covering the respiratory epithelium of the deep lung is the first biological barrier encountered by nanoparticles after inhalation. We here report for the first time significant differences for metal oxide nanoparticles to the binding of surfactant protein A (SP-A), the predominant protein component of ALF. SP-A is a physiologically most relevant protein and provides important biological signals. Also, it is involved in the lung's immune defence, controlling e.g. particle binding, uptake or transcytosis by epithelial cells and macrophages. In our study, we could prove different particle–protein interaction for eight different nanoparticles, whereas particles of the same bulk material revealed different adsorption patterns. In contrast to other proteins as bovine serum albumin (BSA), SP-A does not seem to significantly deagglomerate large agglomerates of particles, indicating different adsorption mechanisms as in the well-investigated model protein BSA. These findings may have important consequences for biological fate and toxicological effects of inhaled nanomaterials.

1. Introduction

When nanoparticles come into contact with biological systems, their interactions with proteins is of utmost importance. As it is known that small particles are taken up in higher amounts than larger ones, the level of particle uptake into cells could be altered due to protein coating of particles. Dispersion of nanoparticles in protein solution can drastically alter the dispersion characteristics, leading to either increased or decreased particle sizes. We have previously demonstrated that the addition of fetal calf serum leads to deagglomeration [1] and hence to smaller particle sizes for some of the particles tested here. Also, it could be demonstrated by Ehrenberg and co-workers that particles coated with serum proteins adsorbed onto endothelial cells in higher amounts as uncoated ones [2]. Hence, the phenomenon of protein adsorption onto nanoparticles entering biological systems could lead to significant toxicological consequences and must be investigated thoroughly.

The Dawson group has pioneered structure–property relationships in protein coronas during the last few years using plasma proteins [3–6]. However, there is general consensus in nanotoxicology that inhalation represents the most relevant route of exposure [7]. In this case, the first biological barrier that inhaled particles will encounter is the pulmonary surfactant on top of the alveolar lining fluid (ALF), an ultra thin liquid layer covering the respiratory epithelium towards the air side. The pulmonary surfactant consists of approximately 90% lipids (mainly phospholipids) and 10% proteins (so-called surfactant proteins, SP) by weight [8]. Concerning the interaction between the pulmonary surfactant and inhaled particles, we assume that especially the four so-called lung surfactant proteins play a key role. Surfactant protein B and C are very lipophilic and improve the surface activity of surfactant phospholipids [9]. The more hydrophilic surfactant proteins A and D (SP-A, SP-D) belong to the collectins recognizing, binding and facilitating the clearance of infectious particles from the lung [10]. As SP-A is the most prominent of the four surfactant proteins and because of its major role in lung immune defence, a possible particle interaction with this protein is highly important to understand and to predict further biological responses. The adsorption of pulmonary surfactant components has already been addressed in several studies for diesel soot, quartz and kaolin [11] as well as for gold [12], TiO_2 and polystyrene nanoparticles [13,14] but they predominantly concentrated on the lipid fraction of pulmonary

Abbreviations: ALF, alveolar lining fluid; SP-A, surfactant protein A; BSA, bovine serum albumin; pBALF, porcine broncheoalveolar lavage fluid; BCA assay, bicinchinoninic acid protein quantification assay; AUC, analytical ultracentrifugation; CRD, carbohydrate recognition domains; SDS–PAGE, sodiumdodecylsulfate–polyacryl-gelelectrophoresis; SPs, surfactant proteins; FCS, fetal calf serum; CNTs, carbonanotubes.

* Corresponding author. Department of Biopharmaceutics and Pharmaceutical Technology, Saarland University, D-66041 Saarbruecken, Germany. Tel.: +49 681 302 2039; fax: +49 681 302 4677.

E-mail addresses: chr.schulze@mx.uni-saarland.de (C. Schulze), ufs@mx.uni-saarland.de (U.F. Schaefer), c.ruge@mx.uni-saarland.de (C.A. Ruge), wendel.wohlleben@basf.com (W. Wohlleben), lehr@mx.uni-saarland.de (C.-M. Lehr).

0939-6411/$ - see front matter © 2010 Elsevier B.V. All rights reserved.
doi:10.1016/j.ejpb.2010.10.013

surfactant. Also, with the exception of TiO_2, quartz and kaolin, those particles are hardly transferable to materials that are handled at kiloton scale already, such as metal oxide nanoparticles. Therefore, we decided to study the interaction of metal oxide nanoparticles with lung surfactant protein A present in porcine broncheoalveolar lavage fluid (pBALF), as pBALF is a well known and widely used source for surfactant proteins.

To investigate nanoparticles–protein interactions, microcalorimetry and surface plasmon resonance technique were introduced by Cedervall et al. using co-polymer particles as model [15]. However, we found these techniques not readily transferable to industrially relevant nanomaterials, such as metal oxides, mainly due to rapid sedimentation. Hence, we adopted the colorimetric bicinchinoninic acid protein quantification assay (BCA assay), gel electrophoresis and immunoblotting to quantify and identify the interacting proteins.

2. Materials and methods

2.1. Determination of protein adsorption onto metal oxide nanoparticles via BCA assay

One hundred and forty-eight milligrams of nanoparticles was dispersed with 2 ml of a 1:10 diluted pBALF solution (leading to a protein concentration of 7.4 mg/ml; preparation see section 1b), leading to particle–protein ratio of 10:1. The resulting dispersions were stirred at room temperature for 1 h at 300 rpm, transferred into Eppendorf tubes and centrifuged at 23,000*g* for 45 min at 10 °C in a Hettich Universal 30 RF with rotor E1175. Afterwards, the supernatants were used for BCA assay as described in the manual (Bicinchinoninic Acid Kit for Protein Determination, Sigma, Cat. No. BCA1-1KT). The resulting protein concentrations in the supernatants were subtracted from the original concentration and related to the negative control (centrifuged protein solution without particles).

2.2. Preparation of porcine broncheoalveolar lavage fluid (pBALF)

pBALF preparation was modified after Taeusch et al. [55]. In short, three porcine lungs, derived from a local butcher and removed in toto, were each filled with about 0.6 l of cold (4 °C) purified water and gently massaged for about 5 min. We used water instead of buffer to avoid any influence of salts onto the adsorption process. Then, the fluid was removed and collected; the fluid of all lungs was pooled and centrifuged at 1400 rpm for 4 min to remove cellular residues. The thus obtained volume of about 2 l of pBALF was frozen at −80 °C until lyophilisation in a Christ Alpha 2-4 LSC lyophilisation device and rediluted in 200 ml of purified water in order to concentrate the proteins. The protein content was determined with BCA assay to be 74.03 mg/ml. The content of SP-A was proven by western blotting and immunostaining, performed as described later, in comparison with literature [17,49] and a SP-A reference. The pBALF was aliquoted and stored at −80 °C until use.

The time frame between picking up the lungs and preparation of the pBALF was about 45 min. During the whole transportation process, the lungs were cooled on ice to preserve the tissue. After they arrived in the laboratory, we started pBALF preparation immediately.

2.3. SDS–PAGE, western blotting and immunostaining

The contents and preparation of all buffers and solutions are summarized in Table 1. After incubation with the nanoparticles in a particle–protein relation of 10:1 and centrifugation as described for BCA assay, the supernatants were removed, the pellets rinsed three times with purified water and resuspended with 0.5 ml of purified water. A volume of 0.1 ml of the supernatants and pellet dispersions, respectively, was mixed with 0.1 ml of 2x sample buffer and denatured for 5 min at 95 °C to detach the proteins from the particles. Then, 20 μl of each sample was applied to a 12% polyacrylamide gel (4.5 ml of purified water, 2.5 ml of separating gel buffer, 3 ml of acrylamide solution (Rotiphorese Gel 40 (29:1), Carl Roth GmbH & Co, Cat. No. A515.1), 0.05 ml of ammoniumperoxodisulfate (APS; Carl Roth GmbH & Co, at. No. 95923), 0.005 ml of Temed (Carl Roth GmbH & Co, Cat. No. 23673)), covered with a 4% stacking gel (2.5 ml of purified water, 0.95 ml of stacking gel buffer, 0.4 ml of acrylamide solution, 0.0225 ml of APS, 0.0075 ml of Temed) and run, soaked in running buffer, for 110 min at 100 V in a BioRad MiniProtean II.

The stacking gels were removed and the separating gels covered with nitrocellulose membranes (Protran BA 85 Nitrocellulose, Whatman, Cat. No. 10401197), sandwiched in filter paper and soaked in blotting buffer. After removing air bubbles from the layer interspaces, the blotting sandwiches were transferred into a Bio-Rad Mini Trans-blot Cell and tank-blotted in blotting buffer at 300 mA for 90 min. As the protein marker (Spectra Multicolor, Broad Range Protein Ladder, Fermentas, Cat. No. SM1849) was prestained, there was no need to check the protein transfer by Ponceau staining.

The membranes were blocked for 2 h in blocking buffer and then they were incubated with rabbit anti-surfactant protein A at a dilution of 1:2500 in blocking buffer (Anti-Surfactant Protein A, Millipore, Cat. No. AB 3424) for 2 h under gentle luffing. The blots were washed three times with TBS buffer for 10 min prior to incubation with alkaline phosphatase–conjugated goat anti-rabbit IgG (Goat anti-Rabbit IgG, Alkaline Phosphatase Conjugated, Millipore, Cat. No. AP132A) and diluted 1:5000 in blocking buffer. After washing three times for 10 min with TBS buffer, the blots were developed in 10 ml of NBT-BCIP dying solution for several minutes. Finally, the blots were scanned and saved as .tiff files.

2.4. Agglomeration control by analytical ultracentrifugation (AUC)

The particle size distribution was determined by analytical ultracentrifugation (AUC) of ~500 μL of the test dispersion with a mass ratio of nanomaterial:BALF proteins = 2:1. This ratio corresponds to around 10 mg/cm^2 protein mass concentration per nanomaterial surface for the metal oxides, because these have all similar values of the BET surface. This ratio in the solution was chosen because this situation is close to a particulate contamination, in the sense that the reservoir of surfactant proteins is not depleted: Only a small part of the available protein mass has adsorbed.

Simultaneous detection by synchronized interference optics (Beckmann, model XLI) quantified the amount and the diameter of each fraction independently from 1 nm up to several microns diameter [7,56,57]. We can thus successively quantify in a single measurement the protein content, the protein molar mass, the nanomaterial content and the nanomaterial state of agglomeration, presented as double-logarithmic plot in Fig. 2. When the retrieved concentration of proteins is less than 100 wt% at the expected molar mass, we assume that the remaining proteins have adsorbed to a particulate surface. When the retrieved concentration of nanomaterial is less than 100 wt% in the measurement interval, we assume that the remainder has agglomerated. The evaluation of the AUC raw data incorporated the fractal morphology of nanoparticle agglomerates and applied the fractional dimension of 2.1 together with the sedimentation relation as specified in Eq. (6) of Ref. [58]. This value of the fractional dimension has been shown to be universal for all reaction-limited colloid agglomerates

Table 1
Buffers and solutions needed for SDS–PAGE, western blotting and immunostaining. This table contains all chemicals used to create the buffers for the performed gel electrophoresis and immunostaining.

	Components	Concentration
Stacking gel buffer	Tris–HCl (Sigma, T1503) **S**odium**d**odecyl**s**ulfate (SDS; Serva Electrophoresis GmbH, Cat. No. 20783) adjust to pH 6.8	0.5 M 0.4% (w/v)
Separation gel buffer	Tris–HCl (Sigma, T1503) SDS (Serva Electrophoresis GmbH, Cat. No. 20783) adjust to pH 8.8	1.5 M 0.4% (w/v)
2× Sample buffer	Tris–HCl (Sigma, T1503) SDS (Serva Electrophoresis GmbH, Cat. No. 20783) Glycerin (Sigma, G8773) β-Mercaptoethanol (Sigma, M7522) Bromphenol blue (Pharmacia Biotech, plusone, Cat. No. 17-1329-01) adjust to pH 6.8	0.12 M 8% (w/v) 20% (w/v) 10% (v/v) 0.1% (w/v)
Running buffer	Tris (Sigma, T1503) Glycin (Carl Roth GmbH & Co, Cat. No. 3908.2) SDS (Serva Electrophoresis GmbH, Cat. No. 20783)	0.025 M 0.192 M 0.1% (w/v)
Blotting buffer	Tris–HCl (Sigma, T1503) Glycin (Carl Roth GmbH & Co, Cat. No. 3908.2) Methanol (Fisher Scientific, HPLC grade, Cat. No. M/4056/17) pH 8.3	0.025 M 0.192 M 20% (v/v)
TBS buffer	Tris–HCl (Sigma, T1503) NaCl (Sigma, S5886) pH 7.5	0.02 M 0.15 M
Blocking solution	Low-fat milk (1.5% fat; local dairy) TWEEN 80 (Sigma, P4780) in TBS buffer	10% (v/v) 0.1% (v/v)
Buffer for NTB/BCIP dying solution	Tris–HCl (Sigma, T1503) NaCl (Sigma, S5886) $MgCl_2$ (Sigma, M4880) pH 9.5	0.1 M 0.1 M 0.05 M
NTB/BCIP dying solution	NTB/BCIP stock solution (Roche Diagnostics GmbH, Cat. No. 11681451001) in buffer for NTB/BCIP dying solution	0.2% (v/v)

[58,59]. The tabulated material's constant of refractive index allows the interference optics to linearly directly quantify the fraction that is dispersed to diameters below 100 nm in the actual test preparation, with the full size distributions shown in the integrated table in Fig. 3. The value for the nanodispersed fraction is regarded as an upper limit, judging from the comparison of size determination methods with different physical measurement principles [1].

2.5. Particle properties

To be able to interpret the protein adsorption patterns and to show the high variability of the particles we were dealing with, we tried to characterize the nanoparticles we worked with. TEM images were carried out after dispersion in isopropanol and drying before use (see Fig. 1).

3. Results and discussion

3.1. Direct and indirect analysis of SP-A adsorption onto metal oxide nanoparticles

To evaluate the interactions of metal oxide nanoparticles with the lung surfactant proteins, we stirred the particles into pBALF. The powder hits an air–liquid interface first, where phospholipids may be their first encounter, but the natural timescale of wetting is disturbed by enforced mixing. Although this simplified (but reliable) procedure does not exactly mimic the landing of inhaled particles onto the alveolar lining fluid, it is relevant for the situation when the particles have sunk into the ALF already and reached the aqueous subphase.

Protein adsorption on nanoparticles was determined by measuring the protein content in the supernatant (BCA assay) and expressed as a percentage of the protein content in a similarly treated pBALF sample without nanoparticles. Clearly, different particles show a different protein adsorption (see Fig. 2a); $BaSO_4$ and TiO_2 A are generally adsorbing much less protein than the rest of the particles tested. Also, different particles of the same bulk material reveal different adsorption patterns, as could be shown for CeO_2 A and B compared to CeO_2 C and for the two TiO_2 particles.

As SP-A is by far the most abundant of the surfactant proteins [16–18] and specific antibodies are commercially available, we decided to focus our further experiments on SP-A. SP-A consists of eight trimers, each of those trimers including a long triple-helical collagenous stem, a flexible hinge, a helical bundle connector and a globular head [19–21]. This globular structure contains carbohydrate recognition domains (CRD), and as SP-A is a member of the collectin protein family, it recognizes and binds carbohydrates in a Ca^{2+}-dependent process as a part of the immune defence system [22,23]. Also, SP-A is able to bind multiple ligands as sugars, Ca^{2+} and phospholipids in a cooperative manner [19], allowing SP-A to bind to the surface of multiple pathogens like bacteria, viruses and fungi [10], but also associates with pulmonary surfactant membranes via the CRD [24,25].

Prior to adsorption experiments, the presence of SP-A in pBALF was confirmed by immunoblotting (data not shown). To measure the binding of SP-A onto the metal oxide nanoparticles, samples of both the supernatant and the pellet of the previously described adsorption experiment were each analyzed by SDS–PAGE under reducing conditions, followed by western blot and immunostaining (Fig. 2b).

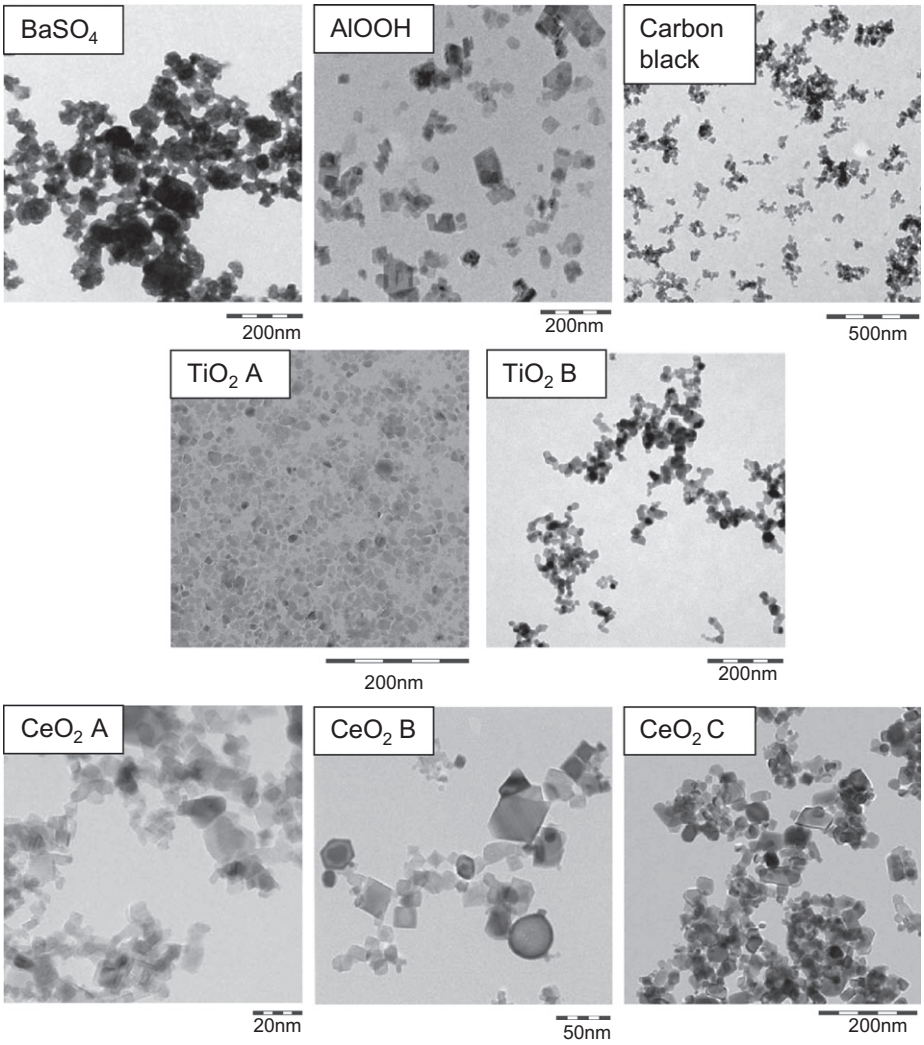

Fig. 1. TEM pictures of the different nanoparticles tested for protein adsorption. The particles were dispersed in isopropanol and dried before use.

TiO_2 A and $BaSO_4$ showed relatively low overall protein adsorption (30% and 5%, resp.), but nevertheless high SP-A interaction as suggested by a strong SP-A signal in the pellet and a weak (TiO_2 A) or no ($BaSO_4$) signal in the supernatant. Obviously, those particles are adsorbing SP-A very specifically. For the model protein bovine serum albumin (BSA), protein adsorption has been reported to be pH dependent, the maximum being near to the isoelectric point [26,27]. This, however, might be not transferable to the adsorption of SP-A onto $BaSO_4$, as the pH of the $BaSO_4$ dispersion of 8.6 differs from the pI of SP-A of 4.4-5.6. Interestingly, according to the manufactureŕs specifications, both TiO_2 A and $BaSO_4$ bear some organic modifications (Table 2). As pBALF is not Ca^{2+} free, an ion-mediated adsorption to the organic groups of the two particles via the CRD domain of SP-A may be possible, similarly as has been suspected by Salvador-Morales and co-workers for accidental organic modifications of carbon nanotubes [28].

AlOOH and CeO_2 C show an intermediate overall binding of pBALF proteins (Fig. 2a). In contrast, binding of SP-A to CeO_2 C was only weak, as indicated by the fact that the strongest signal was found in the supernatant and the weaker signal in the pellet. For AlOOH, SP-A was only detected in the pellet, similar as for $BaSO_4$.

Strongest (~100%) overall protein binding in pBALF was observed with TiO_2 B, CeO_2 A and B and carbon black. For neither of those particles, any SP-A signal could be detected in the supernatant. For TiO_2 B and CeO_2 B, similar SP-A adsorption to the nanoparticles was observed (intermediate SP-A signal in the pellet). Only a very weak SP-A signal was found for CeO_2 A pellet, whereas carbon black revealed no SP-A signal at all. The higher the adsorption of different proteins, the higher is the possibility of protein–protein interactions, e.g. via hydrogen bonds. As the overall protein binding for TiO_2 B, CeO_2 A and B and carbon black is nearly total, the possibility of not only protein–particle but also protein–protein interaction is given. If this was the case, the protein–protein interactions should be disturbed by the denaturation and reduction process prior to the gel electrophoresis, and therefore, a SP-A signal should be found in the desorbed proteins from the pellet. However, this is not the case. Instead, SDS–PAGE and Coomassie staining still shows some protein bands for all particle pellets, except for carbon black, proving the detachment procedure is working for most proteins (data not shown). Notably, the SP-A signals of the pellets compared to the supernatants are not correlating for TiO_2 B, CeO_2 A and B and carbon black. The reason might be an extremely strong binding of SP-A to the surface of those types of nanoparticles, even resisting the conditions of the desorption protocol used in this study. As we stated previously, the globular domains of SP-A do not only bind to carbohydrates, but also to phospholipids. Although this interaction is considered superficial, it has hydrophobic and polar contributions [19]. As carbon black is very hydrophobic, a hydrophobic interaction between carbon black and the

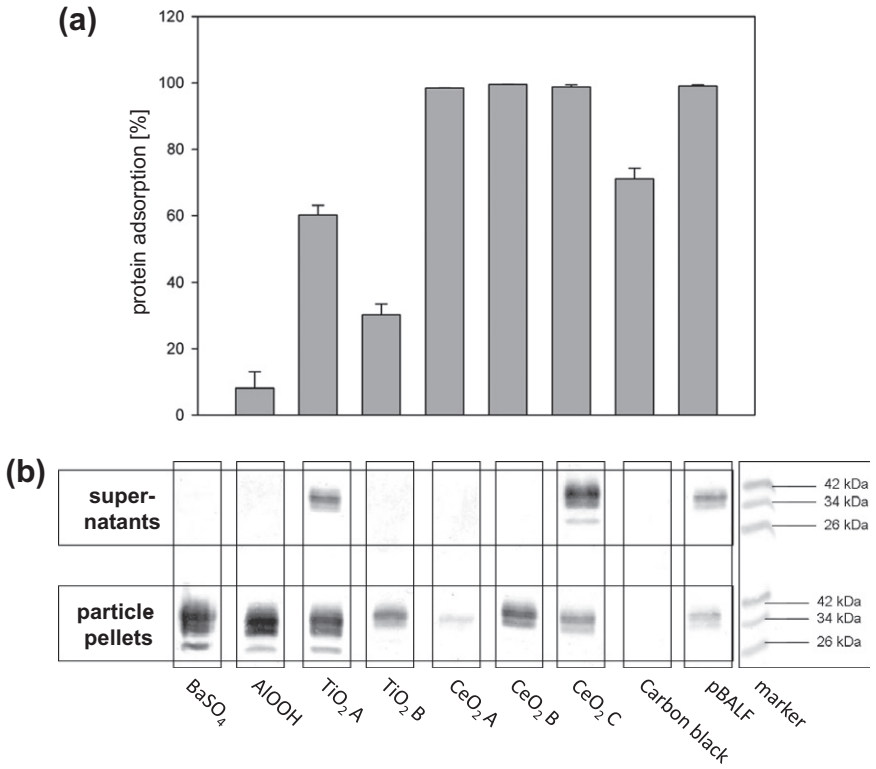

Fig. 2. Adsorption of proteins from pBALF at a nanoparticle/protein ratio of 10:1. (a) Total protein adsorption (BCA assay): The particles show striking differences, even when derived from the same bulk material. All values were related to the pBALF-supernatant after nanoparticle separation by centrifugation (mean + standard deviation; $n = 3$). (b) Immunoblot of SP-A from supernatant and pelleted nanoparticles after conditioning in pBALF (SP-A monomer: 36 kDa). As control, pBALF 1:10 diluted was used ($n = 3$).

Table 2
Physico-chemical properties of the nanoparticles tested. This table summarizes the physico-chemical properties of the tested metal oxide nanoparticles. #pH measurements were taken with 10 mg/ml nanoparticle in purified water.

Sample	Chemical composition, crystallinity	Mean primary particle size, morphology	Surface area [m^2/g]	Surface chemistry [At%]	Organic modification	pH#
$BaSO_4$	56.5% Ba 38.6% SO_4 orthorhombic	38 nm irregular but globular	41.4	Ba 13 S 11 O 52 C 17	Yes	8.6
AlOOH	82.7% AlOOH; impurities: C, Na, Fe, Si, Li, B	40 nm, irregular but spherical	47	O 62 Al 32 C 7	None	4.3
TiO_2 A	O 58% Ti 41% Cl > 1% anatase 95%, rutile 5%	17 nm irregular but spherical	117	O 53 Ti 21 C 25 Cl 1	Yes	5.4
TiO_2 B	>99.5% TiO_2 rutile and anatase, tetragonal	27 nm irregular but globular	52	O 58 Ti 26 C 14 N 0.5 Cl 1	None	6.1
CeO_2 A	>99.97% purity	14 nm cubic, aggregated	63	O 57 Ce 25 C 18	None	5.9
CeO_2 B	>99.97% purity	20 nm, aggregated	44	O 56 Ce 22 C 22	None	6.2
CeO_2 C	>99% CeO_2 Cerianite, cubic	70 nm irregular but globular	33	O 53 Ce 26 C 20 Cl 0.6	None	5.9
Carbon black	n.d.	16 nm, aggregated	340	n.d.	None	5

globular side of SP-A might be speculated, boosted by the largest BET surface of all particles tested (340 m^2/g). This also adds to the high affinity of overall protein binding, causing failure of the desorption protocol and hence empty lanes on the gels for both supernatant and pellet.

It is known that protein adsorption is depending on the hydrophobicity of the particle surface [29–31]. As stated previously, 90 wt% of ALF are (phospho)lipids and we probably washed out this lipid fraction into our pBALF at least partially. Hence, an indirect adsorption mechanism, mediated or influenced by those lipids, is most likely.

Comparing the binding of pBALF proteins and in particular SP-A to the different nanomaterials in this study, we could observe striking differences, even for nanoparticles made of the same material (e.g. CeO_2 A versus B or C; TiO_2 A versus B). There was no obvious correlation with physico-chemical data such as the mean primary particle size, surface area, etc. (Table 2), which would allow a prediction of protein binding from such data.

3.2. Investigation of deagglomeration capacity of pBALF

Complementary to protein binding, we also studied the agglomeration behaviour of the same particles in pBALF, the second property that decides about a nanoparticle's trafficking in the body. Analytical ultracentrifugation (AUC) with interference detection provides a signal that is directly linear with the concentration in the measurement interval [7]. The ultrafine fraction (below 100 nm diameter) can be quantified. In Fig. 3, the resulting particle size distributions are shown with logarithmic axes.

Only TiO_2 A and $BaSO_4$ are dispersable by stirring in water with 40 wt% and 0.5 wt% ultrafine fraction, respectively. For the more hydrophobic nanomaterials (carbon black, unfunctionalized metal oxides), less than 0.01 wt% ultrafine fraction is found in water, but media with serum or SPs enhance wetting and lower the degree of agglomeration. The detailed size distributions (Fig. 3) indicate that agglomeration tendency in pBALF is still significantly stronger than in fetal calf serum (FCS; Fig. 3), which is widely used in cell culture media. Several studies have hinted at the dispersing power of albumin and other interface-active serum components on CNTs [32–34], metal carbide nanoparticles [35,36] and metal oxide nanoparticles[1,35–38]. For mouse BALF, the degree of agglomeration of metal oxide nanoparticles was reported to be comparable with a buffer containing BSA and dipalmitoyl phosphatidyl choline [39] and in a BAL-mimicking dispersion medium [40], but only after 10 min. ultrasonication. Obviously, the anticipated interface activity of SPs is in general not sufficiently strong to overcome the agglomeration or flocculation tendency due to other components in complete pBALF. This result is in good agreement with histological studies of lung slices after inhalation exposure of rodents, where the particulate material that was deposited on the lung surface is found in the form of agglomerates [41]. As one function of SP-A is the aggregation of bacteria via its CRD [22], this behaviour is logic and points to different adsorption mechanisms compared to BSA.

After inhalation and deposition in the deep lung, i.e. ALF, particles with a diameter of 1–6 μm are wetted and sink into the aqueous phase [42], whereas this mechanism is independent of shape, surface topography and surface free energy [43–46]. This process becomes even more efficient with decreasing particle size, and this is expected to occur with nanoparticles, too [47]. As SP-A is integrated into the lipid structure of pulmonary surfactant, the tested nanoparticles most likely come in contact with SP-A *in vivo*.

Our results clearly show that there are specific differences in the binding and interaction of metal oxide nanoparticles with SP-A. A major biological role of SP-A is to bind to inhaled particulate matter (e.g. microorganisms, dust) to enhance their phagocytic clearance by macrophages [28,48,49]. In this way, SP-A plays an important role in limiting pulmonary infection, lung allergy and inflammation [50]. On the one hand, the binding pattern of SP-A and other lung surfactant proteins may be decisive whether inhaled particles will be phagocytosed by macrophages and hence cleared from the deep lung to the airways. Although Geiser and colleagues found that lung surface macrophages do not efficiently phagocytose these ultrafines but take them up in a rather sporadic and unspecific way [51], most of our particles were highly agglomerated and thus still large enough for this clearance pathway.

On the other hand, uptake and hence translocation of particles might be facilitated, as Type II cells, which cover the majority of the alveolar region, have SP-A receptors that cause phospholipid uptake [52]. Nanoparticles could be taken up "accidentally" via this surfactant trafficking. This theory is supported by data from *in vivo* experiments that also indicate nanoparticle uptake into epithelia of the respiratory tract via transcytosis and translocation into the lymphatic system or the blood stream [53].

In another way, the interaction of SP-A with inhaled metal oxide nanoparticles could be important, as a relative SP-A deficiency could occur due to its accumulation onto particles. SP-A knockout mice are less effective in clearing lung pathogens, and therefore, these mice are more susceptible to lung infection. SP-A-deficient animals also present decreased phagocytosis and oxidant metabolism in response to instilled Group B streptococci [54]. There are even a few publications indicating disease correlation with lowered levels of SP-A in humans. These include association of lowered SP-A levels with asthma and allergen-induced bronchial inflammation [22,23]. Obviously, there are strong reasons to assume that the binding to SP-A, and probably other lung surfactant

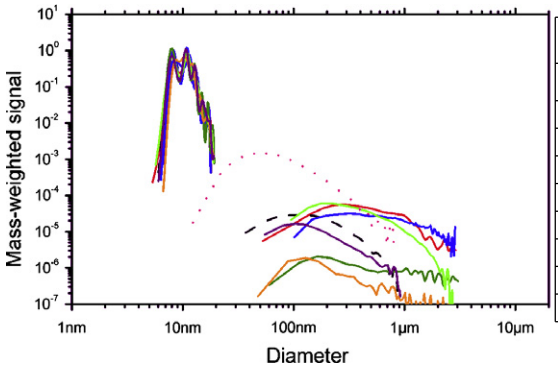

		Fraction of particles < 100 nm [wt%]	
	particle	pBALF	FCS
– –	$BaSO_4$	6	10.4
	AlOOH	0.7	1.2
· · · ·	TiO_2 A	30	38
	TiO_2 B	0.07	0.05
	CeO_2 A	0.1	12.9
	CeO_2 B	0.2	13
	CeO_2 C	1.9	0.12
	Carbon Black	0.05	0.07

Fig. 3. Full particle size distribution of nanoparticles in diluted pBALF from interference AUC. The tables show the initial weight ratio and the protein and particle concentrations within the shown size interval as well as the resultant ultra fine fraction of the particle suspension.

proteins as well, can alter the toxicological properties of particulate matter, such as metal oxide nanoparticles, reaching the deep lung after inhalation drastically.

Strikingly, only the two particles that were organically functionalized with synthetic polymers ($BaSO_4$ powder and TiO_2 A) did not almost completely agglomerate after pBALF exposure. These are the same particles that differentiated by low overall protein adsorption, but strong SP-A interaction (see Fig. 2b). This points again to the decisive role of the surface chemistry in nanotoxicology and opens routes to control the fate of nanomaterials in the lung.

4. Conclusions

In this study, for the first time, differences in the interaction of industrially relevant metal oxide nanoparticles with physiologically relevant lung surfactant protein A were demonstrated. Attempts to correlate the adsorption patterns of SP-A with those of commonly used model proteins (e.g. BSA) failed, underscoring the need to apply sufficiently specific and sensitive analytical methods. In the future, further adsorption experiments with all four surfactant proteins must be performed to find out more about the structure activity relations between particles and their binding of lung surfactant proteins. Also, the effects of lung surfactant protein adsorption onto particles and their biological properties, in particular alveolar clearance by macrophages and translocation across the alveolar epithelium, must be investigated.

5. Competing interests

The authors declare that they have no competing interests.

Acknowledgements

We thank the Federal Ministry of Education and Research BMBF (Project "NanoCare", Förderkennzeichen 03X0021C) for financial funding. Andreas Henning is thanked for his help preparing pBALF solution. Especially, we thank the industrial partners of NanoCare, i.e. Evonik Degussa GmbH, Bayer Material Science AG, ItN Nanovation AG and Solvay Infra Bad Hönningen GmbH, for providing the nanomaterials and the physico-chemical data for the particles used.

References

[1] C. Schulze, A. Kroll, C.M. Lehr, U.F. Schaefer, K. Becker, J. Schnekenburger, C. Schulze Isfort, R. Landsiedel, W. Wohlleben, Not ready to use – overcoming pitfalls when dispersing nanoparticles in physiological media, Nanotoxicology 2 (2008) 51–61.
[2] M.S. Ehrenberg, A.E. Friedman, J.N. Finkelstein, G. Oberdorster, J.L. McGrath, The influence of protein adsorption on nanoparticle association with cultured endothelial cells, Biomaterials 30 (2009) 603–610.
[3] S. Lindman, I. Lynch, E. Thulin, H. Nilsson, K.A. Dawson, S. Linse, Systematic investigation of the thermodynamics of HSA adsorption to N-isopropylacrylamide/N-tert-butylacrylamide copolymer nanoparticles. Effects of particle size and hydrophobicity, Nano Letters 7 (2007) 914–920.
[4] M. Lundqvist, J. Stigler, G. Elia, I. Lynch, T. Cedervall, K.A. Dawson, Nanoparticle size and surface properties determine the protein corona with possible implications for biological impacts, Proceedings of the National Academy of Sciences of the United States of America 105 (2008) 14265–14270.
[5] I. Lynch, T. Cedervall, M. Lundqvist, C. Cabaleiro-Lago, S. Linse, K.A. Dawson, The nanoparticle-protein complex as a biological entity; a complex fluids and surface science challenge for the 21st century, Advances in Colloid and Interface Science 134-135 (2007) 167–174.
[6] I. Lynch, K.A. Dawson, Protein–nanoparticle interactions, Nano Today 3 (2008) 40–47.
[7] R. Landsiedel, L. Ma-Hock, A. Kroll, D. Hahn, J. Schnekenburger, K. Wiench, W. Wohlleben, Testing metal-oxide nanomaterials for human safety, Advanced Materials 22 (2010) 2601–2627.
[8] J. Goerke, Pulmonary surfactant: functions and molecular composition, Biochimica et biophysica acta 1408 (1998) 79–89.
[9] R.L. Bissinger, C.A. Carlson, Surfactant, Newborn and Infant Nursing Reviews 6 (2006) 87–93.
[10] P.S. Kingma, J.A. Whitsett, In defense of the lung: surfactant protein A and surfactant protein D, Current Opinion in Pharmacology 6 (2006) 277–283.
[11] W.E. Wallace, M.J. Keane, D.K. Murray, W.P. Chisholm, A.D. Maynard, T.M. Ong, Phospholipid lung surfactant and nanoparticle surface toxicity: lessons from diesel soots and silicate dusts, Journal of Nanoparticle Research 9 (2007) 23–38.
[12] M.S. Bakshi, L. Zhao, R. Smith, F. Possmayer, N.O. Petersen, Metal nanoparticle pollutants interfere with pulmonary surfactant function in vitro, Biophysical Journal 94 (2008) 855–868.
[13] C. Schleh, J.M. Hohlfeld, Interaction of nanoparticles with the pulmonary surfactant system, Inhalation Toxicology 21 (Suppl 1) (2009) 97–103.
[14] C. Schleh, C. Muhlfeld, K. Pulskamp, A. Schmiedl, M. Nassimi, H.D. Lauenstein, A. Braun, N. Krug, V.J. Erpenbeck, J.M. Hohlfeld, The effect of titanium dioxide nanoparticles on pulmonary surfactant function and ultrastructure, Respiratory Research 10 (2009) 90.
[15] T. Cedervall, I. Lynch, S. Lindman, T. Bergga?rd, E. Thulin, H. Nilsson, K.A. Dawson, S. Linse, Understanding the nanoparticle-protein corona using methods to quntify exchange rates and affinities of proteins for nanoparticles, Proceedings of the National Academy of Sciences of the United States of America 104 (2007) 2050–2055.
[16] S. Matalon, J.M. Hickman-Davis, J.R. Wright, J.L. Geoffrey, D.S. Steven, SURFACTANT | Surfactant Protein A (SP-A), in: Encyclopedia of Respiratory Medicine, Academic Press, Oxford, 2006, pp. 143–148.
[17] F.X. McCormack, Structure, processing and properties of surfactant protein A, Biochimica et biophysica acta 1408 (1998) 109–131.
[18] R.H. Notter, P.R. Chess, Z. Wang, J.L. Geoffrey, D.S. Steven, SURFACTANT | Overview, in: Encyclopedia of Respiratory Medicine, Academic Press, Oxford, 2006, pp. 135–143.
[19] C. Casals, Role of surfactant protein A (SP-A)/lipid interactions for SP-A functions in the lung, Pediatric Pathology and Molecular Medicine 20 (2001) 249–268.
[20] H.P. Haagsman, Structural and functional aspects of the collectin SP-A, Immunobiology 205 (2002) 476–489.
[21] S. Heinrich, D. Hartl, M. Griese, Surfactant protein A – from genes to human lung diseases, Current Medicinal Chemistry 13 (2006) 3239–3252.
[22] T.P. Hickling, H. Clark, R. Malhotra, R.B. Sim, Collectins and their role in lung immunity, Journal of Leukocyte Biology 75 (2004) 27–33.
[23] J.M. Hohlfeld, The role of surfactant in asthma, Respiratory Research 3 (2002) 4.
[24] N. Palaniyar, M. Ikegami, T. Korfhagen, J. Whitsett, F.X. McCormack, Domains of surfactant protein A that affect protein oligomerization, lipid structure and surface tension, Comparative Biochemistry and Physiology – A Molecular and Integrative Physiology 129 (2001) 109–127.
[25] N. Palaniyar, R.A. Ridsdale, F. Possmayer, G. Harauz, Surfactant protein A (SP-A) forms a novel supraquaternary structure in the form of fibers, Biochemical and Biophysical Research Communications 250 (1998) 131–136.
[26] Y.-Y. Liang, L.-M. Zhang, W. Li, R.-F. Chen, Polysaccharide-modified iron oxide nanoparticles as an effective magnetic affinity adsorbent for bovine serum albumin, Colloid and Polymer Science 285 (2007) 1193–1199.
[27] N. Shamim, L. Hong, K. Hidajat, M.S. Uddin, Thermosensitive-polymer-coated magnetic nanoparticles: adsorption and desorption of bovine serum albumin, Journal of Colloid and Interface Science 304 (2006) 1–8.
[28] C. Salvador-Morales, P. Townsend, E. Flahaut, C. Venien-Bryan, A. Vlandas, M.L.H. Green, R.B. Sim, Binding of pulmonary surfactant proteins to carbon nanotubes; potential for damage to lung immune defense mechanisms, Carbon 45 (2007) 607–617.
[29] A. Gessner, R. Waicz, A. Lieske, B. Paulke, K. Mader, R.H. Muller, Nanoparticles with decreasing surface hydrophobicities: influence on plasma protein adsorption, International Journal of Pharmaceutics 196 (2000) 245–249.
[30] J.N. Israelachvili, R.M. Pashley, Measurement of the hydrophobic interaction between two hydrophobic surfaces in aqueous electrolyte solutions, Journal of Colloid and Interface Science 98 (1984) 500–514.
[31] M. Luck, B.R. Paulke, W. Schroder, T. Blunk, R.H. Muller, Analysis of plasma protein adsorption on polymeric nanoparticles with different surface characteristics, Journal of Biomedical Materials Research 39 (1998) 478–485.
[32] L. Lacerda, M.A. Herrero, K. Venner, A. Bianco, M. Prato, K. Kostarelos, Carbon-nanotube shape and individualization critical for renal excretion, Small (Weinheim an der Bergstrasse, Germany) 4 (2008) 1130–1132.
[33] D. Lin, B. Xing, Tannic acid adsorption and its role for stabilizing carbon nanotube suspensions, Environmental Science and Technology 42 (2008) 5917–5923.
[34] D. Nepal, K.E. Geckeler, Proteins and carbon nanotubes: close encounter in water, Small (Weinheim an der Bergstrasse, Germany) 3 (2007) 1259–1265.
[35] S. Bastian, W. Busch, D. Kuhnel, A. Springer, T. Meissner, R. Holke, S. Scholz, M. Iwe, W. Pompe, M. Gelinsky, A. Potthoff, V. Richter, C. Ikonomidou, K. Schirmer, Toxicity of tungsten carbide and cobalt-doped tungsten carbide nanoparticles in mammalian cells in vitro, Environmental Health Perspectives 117 (2009) 530–536.
[36] T. Meissner, A. Potthoff, V. Richter, Suspension characterization as important key for toxicological investigations, Journal of Physics: Conference Series 170 (2009) 6.
[37] P. Bihari, M. Vippola, S. Schultes, M. Praetner, A.G. Khandoga, C.A. Reichel, C. Coester, T. Tuomi, M. Rehberg, F. Krombach, Optimized dispersion of

nanoparticles for biological in vitro and in vivo studies, Particle and Fibre Toxicology 5 (2008).
[38] C.M. Sayes, K.L. Reed, D.B. Warheit, Assessing toxicology of fine and nanoparticles: comparing in vitro measurements to in vivo pulmonary toxicity profiles, Toxicological Sciences 97 (2007) 163–180.
[39] T.M. Sager, D.W. Porter, V.A. Robinson, W.G. Lindsley, D.E. Schwegler-Berry, V. Castranova, Improved method to disperse nanoparticles for in vitro and in vivo investigation of toxicity, Nanotoxicology 1 (2007) 118–129.
[40] D. Porter, K. Sriram, M. Wolfarth, A. Jefferson, D. Schwegler-Berry, M.E. Andrew, V. Castranova, A biocompatible medium for nanoparticle dispersion, Nanotoxicology 2 (2008) 144–154.
[41] L. Ma-Hock, S. Burkhardt, V. Strauss, A.O. Gamer, K. Wiench, B. van Ravenzwaay, R. Landsiedel, Development of a short-term inhalation test in the rat using nano-titanium dioxide as a model substance, Inhalation Toxicology 21 (2009) 102–118.
[42] W.G. Kreyling, M. Geiser, Dosimetry of inhaled nanoparticles, in: J.C. Marijnissen, L. Gradon (Eds.), Nanoparticles in Medicine and Environment, Inhalation and Health Effects, Springer, Berlin, 2009, pp. 145–171.
[43] M. Geiser, M. Matter, I. Maye, V. Im Hof, P. Gehr, S. Schurch, Influence of airspace geometry and surfactant on the retention of man-made vitreous fibers (MMVF 10a), Environmental Health Perspectives 111 (2003) 895–901.
[44] M. Geiser, S. Schurch, P. Gehr, Influence of surface chemistry and topography of particles on their immersion into the lung's surface-lining layer, Journal of Applied Physiology 94 (2003) 1793–1801.
[45] S. Schurch, P. Gehr, V. Im Hof, M. Geiser, F. Green, Surfactant displaces particles toward the epithelium in airways and alveoli, Respiration Physiology 80 (1990) 17–32.
[46] P. Gehr, S. Schürch, Y. Berthiaume, V. Im Hof, M. Geiser, Particle retention in airways by surfactant, Journal of Aerosol Medicine 3 (2009) 27–43.
[47] M. Geiser, W.G. Kreyling, Deposition and biokinetics of inhaled nanoparticles, Part Fibre Toxicol 7 (2010) 2.
[48] K.L. Hartshorn, E. Crouch, M.R. White, M.L. Colamussi, A. Kakkanatt, B. Tauber, V. Shepherd, K.N. Sastry, Pulmonary surfactant proteins A and D enhance neutrophil uptake of bacteria, The American Journal of Physiology 274 (1998) L958–969.
[49] U. Kishore, T.J. Greenhough, P. Waters, A.K. Shrive, R. Ghai, M.F. Kamran, A.L. Bernal, K.B.M. Reid, T. Madan, T. Chakraborty, Surfactant proteins SP-A and SP-D: structure, function and receptors, Molecular Immunology 43 (2006) 1293–1315.
[50] U. Kishore, A.L. Bernal, M.F. Kamran, S. Saxena, M. Singh, P.U. Sarma, T. Madan, T. Chakraborty, Surfactant proteins SP-A and SP-D in human health and disease, Archivum immunologiae et therapiae experimentalis 53 (2005) 399–417.
[51] M. Geiser, M. Casaulta, B. Kupferschmid, H. Schulz, M. Semmler-Behnke, W. Kreyling, The role of macrophages in the clearance of inhaled ultrafine titanium dioxide particles, American Journal of Respiratory Cell and Molecular Biology 38 (2008) 371–376.
[52] P.A. Stevens, H. Wissel, D. Sieger, V. Meienreis-Sudau, B. Rustow, Identification of a new surfactant protein A binding protein at the cell membrane of rat type II pneumocytes, Biochemical Journal 308 (1995) 77–81.
[53] G. Oberdörster, E. Oberdörster, J. Oberdörster, Nanotoxicology: an emerging discipline evolving from studies of ultrafine particles, Environmental Health Perspectives 113 (2005) 823–839.
[54] T.R. Korfhagen, A.M. LeVine, J.A. Whitsett, Surfactant protein A (SP-A) gene targeted mice, Biochimica et biophysica acta 1408 (1998) 296–302.
[55] H.W. Taeusch, J.B. de la Serna, J. Perez-Gil, C. Alonso, J.A. Zasadzinski, Inactivation of pulmonary surfactant due to serum-inhibited adsorption and reversal by hydrophilic polymers: experimental, Biophysical Journal 89 (2005) 1769–1779.
[56] H. Coelfen, Analytical ultracentrifugation of nanoparticles, in: Encyclopedia of Nanoscience and Nanotechnology, American Scientific Publishers, 2004, pp. 67–88.
[57] W. Maechtle, L. Boerger, Analytical Ultracentrifugation of Polymers and Nanoparticles, Springer, Berlin, 2006.
[58] M.Y. Lin, H.M. Lindsay, D.A. Weitz, R.C. Ball, R. Klein, P. Meakin, Universal reaction-limited colloid aggregation, Physical Review 41 (1990) 2005–2020.
[59] D.F. Evans, H. Wennerström, The colloidal domain: where physics, chemistry, biology and technology meet, Wiley, Vch, New York, 1999.